Application of a PCM-rich concrete overlay to control thermal induced curling stresses in concrete pavements

Naser P. Sharifi *, Kamyar C. Mahboub

Department of Civil Engineering, University of Kentucky, Lexington, KY 40506, USA

HIGHLIGHTS

- The weather conditions cause curling stresses in concrete pavements.
- Because of their cyclic nature, they cause fatigue damage in pavements.
- The induced cumulative fatigue Damage Index could be up to 0.22 in a concrete slab.
- Using a thin PCM rich concrete overlay can mitigate this deterioration mechanism.

ARTICLE INFO

ABSTRACT

This study aims to evaluate the application of a Phase Change Material (PCM) rich concrete overlay to reduce curling stresses in concrete pavements. Curling stresses are the results of temperature gradient in pavements, and are comparable to the stresses that are induced by traffic loads. The weather conditions, which have a cyclic nature, are the source of curling stresses, and they cause cyclic tensile and compressive stresses in pavements. This phenomenon causes fatigue damage in concrete pavements and reduces their service life. The PCMs have a high latent heat of fusion and can increase the thermal inertia of concrete. When PCM is used in a concrete overlay, it tends to moderate the temperature gradient in the slab, and thus mitigate the curling stresses. The efficiency of the proposed PCM-rich overlay was evaluated under the real climatic conditions of three different cities in the US. The findings of this research demonstrated that the cumulative fatigue Damage Index (DI) resulted from repetitive curling stresses can be up to 22% in a concrete slab with the service life of 35 years. However, using a 7.6 cm bonded concrete overlay with 25 vol% PCM can moderate the curling stresses so much that the effect of curling induced fatigue damage would be virtually negligible.

1. Introduction

In recent decades, a large number of studies have evaluated the application of Phase Change Materials (PCMs) to improve the thermal performance of buildings and pavements [1,2]. PCMs are substances with high latent heat of fusion, which can go through phase transition cycles without chemical degradation [3]. They can absorb and release a relatively high amount of thermal energy during solid-to-liquid and liquid-to-solid phase transitions; and thus they can work as passive thermal energy storage systems. Various types of PCMs, with a wide range of phase transition temperatures, are industrially available [4]. Their high latent heat of fusion, along with their compatibility with construction and pavement materials

have made PCMs desirable additives to improve thermal properties of these materials [5].

In buildings, incorporation of PCMs in walls and roofs have been reported to be an effective strategy to decrease energy usage for heating and cooling [6,7]. Obviously, less energy usage contributes to a decrease in the emissions such as CO_2 [8]. On the other hand, since the incorporation of PCMs can enhance the thermal inertia of pavement materials, they have been used for different purposes in pavements. Generally, PCMs have been used in pavements in order to decrease freeze/thaw damage in concrete and asphalt pavements [2,9], to assist with melting of ice and snow on concrete pavements [10], and to prevent rutting in asphalt pavements [11]. They have also been used in concrete and asphalt pavements to mitigate the urban heat island effect in large cities [12,13].

Although intensive studies have evaluated different aspects of incorporating PCMs in pavements, the application of PCMs to control curling stresses in concrete pavements has not been studied. Curling

---

* Corresponding author.
E-mail addresses: npsharifi@uky.edu (N.P. Sharifi), kc.mahboub@uky.edu (K.C. Mahboub).

refers to the bending of concrete pavements caused by a temperature gradient [14]. It not only generates bending stresses in the pavement, but also may cause loss of support at slab edges and corners [15]. The magnitude of the thermally induced stresses are comparable to the magnitude of the stresses that are generated in the pavements because of traffic loads [16,17]. However, because the source of curling stresses is the cyclic daily temperature fluctuations, it has a repetitive nature, and the cyclic changes in the induced stresses cause fatigue damage in concrete pavements. Therefore, the goal of this article is to report the findings of a study which investigated the fatigue damage induced in concrete pavements due to curling stresses, and evaluated the effectiveness of PCMs to moderate this type of fatigue damage mechanism.

To do so, the following tasks were carried out: first, real climate data such as air temperature and solar radiation were extracted from TMY3 database [18], and a mathematical model was adopted to calculate surface temperature of concrete pavements for an entire year for various locations with different climatic regions. Second, a 2-D finite element heat transfer model was generated using COMSOL Multiphysics® software package to calculate temperature profile through the cross-section of a pavement. Using these calculations, the most optimum arrangement to incorporate PCMs in the pavement layers was determined. Third, a 3-D finite element stress analysis model using COMSOL software was generated to calculate curling stresses induced in the concrete slab as a result of temperature gradient. Finally, a fatigue damage model for concrete slabs was employed to calculate the fatigue damage induced by the curling stresses over the course of a pavement's service life, and the effectiveness of a PCM-rich concrete overlay to control this damage mechanism was evaluated.

2. Methodology

2.1. Calculation of pavement surface temperature

The first step for calculating temperature profile through the pavement depth is calculating the surface temperature of the pavement. The surface temperature of a pavement is a function of air temperature, solar radiation, wind velocity, and humidity. Surface temperature profile can be drastically different from air temperature profile, and these two temperature profiles cannot be assumed to be the same. Therefore, in this study, a mathematical model was employed to calculate the surface temperature of concrete pavements as a function of climatic data.

Various equations have been proposed for calculating the pavement surface temperature from the climate data [19–21]. There are also some finite difference codes that predict the thermal response of cementitious composites [22]. The humidity of the environment has not been taken into account in many of the proposed equations, because it was found to have negligible effect on the pavement temperature. However, solar radiation has a considerable effect on pavement surface temperature, and has to be taken into account [20]. The adopted equation correlates the surface temperature to air temperature, solar irradiation, and wind velocity. In this correlation, the 24-h periodic temperature of the pavement surface can be calculated by Eq. (1)[1] [21]:

$$T(t) = T_M + T_V \times \frac{H}{\sqrt{(H+C)^2 + C^2}} \times \sin\left(0.262 \times t - \arctan\left(\frac{C}{H+C}\right)\right) \tag{1}$$

---

[1] Since all the parameters and constants presented in the reference of Eq. (1) are in the US customary units, the parameters, constants, and values presented in here and in Table 1 are also only in the US customary units.

where: T(t) = pavement's surface temperature, °F; T_M = mean effective air temperature, °F; T_V = maximum variation in surface temperature from mean, °F; t = time from beginning of cycle, hr; H = h/k, ft^{-1}; h = 1.3 + 0.62 × $W^{0.75}$, surface convection heat transfer coefficient, $BTU/(ft^2 \cdot hr \cdot °F)$; W = wind velocity, mph; k = thermal conductivity of the concrete slab, $BTU/(ft \cdot hr \cdot °F)$; C = $\sqrt{0.131/D}$, ft^{-1}; D = $k/(C_p.\rho)$, concrete slab diffusivity coefficient, ft^2/hr; C_p = concrete slab specific heat, $BTU/(lb \cdot °F)$; and ρ = concrete slab density, lb/ft^3.

In this equation, T_M and T_V can be calculated using the following equations [21]:

$$T_M = T_A + R, T_V = 0.5 \times T_R + 3 \times R \tag{2}$$

where: T_A = daily average air temperature, °F; T_R = daily range in air temperature, °F; R = $(0.67 \times \alpha \times I_0)/h$, average contribution to effective air temperature, °F; α = concrete slab solar absorptivity coefficient, 1; and I_0 = maximum daily solar radiation, $BTU/(ft^2.hr)$.

In Eq. (1), $H/\sqrt{(H+C)^2 + C^2}$ is defined as the modification factor, F; and $\arctan(C/(H+C))$ is defined as the time lag between occurrence of the maximum air temperature and maximum slab's temperature, φ. Therefore. The equation can be rewritten as:

$$T(t) = T_M + T_V \times F \times \sin(0.262 \times t - \varphi). \tag{3}$$

The Eq. (3) approximates the pavement surface temperature by a sinusoidal function. All the physical and thermal properties of the concrete slab, as well as key climate parameters, are involved in this approximation. Therefore, there is a reasonable correlation between the observed and computed surface temperature using this equation [21].

The formulation presented by Eq. (3) was used to calculate the surface temperature of various locations in the US. For each location, air temperature, Global Horizontal Irradiation (GHI), and wind velocity were extracted from TMY3 database [18]. This open-access database has the hourly recorded weather data for 1020 locations in the US. It should be mentioned that in this study, thermal properties of the pavement were modified based on the PCM percentage. Therefore, for each case, the surface temperature of the pavement was calculated using the modified thermal properties of the pavement.

As a demonstration, the weather parameters of the month of November in Lexington, KY (shown in Fig. 1) were applied to a concrete pavement with the parameters presented in Table 1, and the surface temperature of the pavement was calculated. For each day, T_A, T_R, R, T_M, T_V were calculated, and Eq. (1) was used to calculate the surface temperature of the pavement. The comparison between air temperature and calculated pavement surface temperature is shown in Fig. 2. It is worthwhile to mention that for these parameters, φ has been found to be equal to 0.29 Rad; which means the time lag between occurrence of maximum air temperature and maximum pavement temperature is equal to 66 min [21,23].

2.2. Calculation of temperature in the pavement layers

To calculate the temperature changes through the pavement layers, a 2-D finite element heat transfer model using COMSOL software was generated. The physics that were involved in the model were heat conduction, heat convection, and heat radiation. The model also included heat transfer in porous media, and heat transfer with phase change. The concrete slab was modeled as a porous medium so that the PCM could be incorporated inside its porosity. Details regarding the boundary conditions, initial conditions, meshing, etc., as well as the validation process of the model, are provided in another study [24]. In this study, to calculate the temperature profile through the pavement thickness, the thermal properties of the pavement were modified based on the utilized
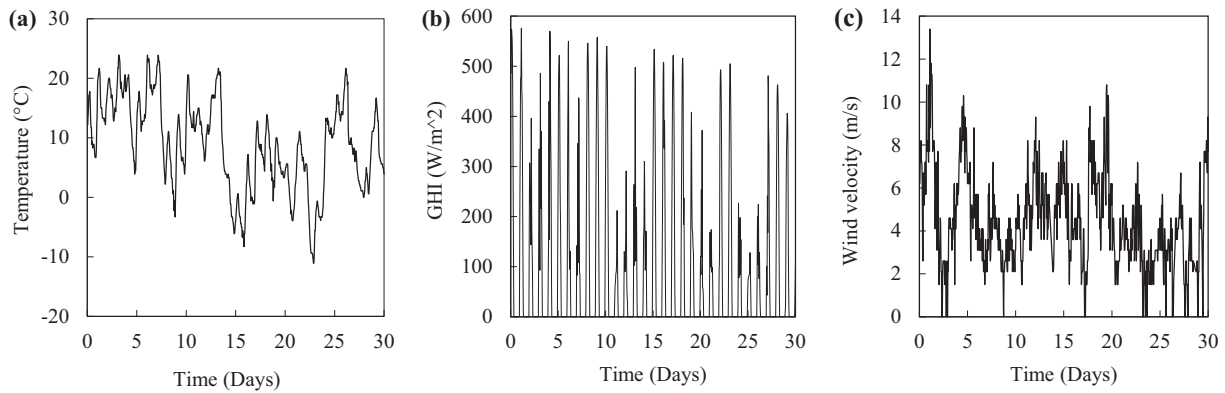
Fig. 1. Weather data of Lexington, KY, in November; obtained from TMY3. a) Air temperature, b) Global Horizontal Irradiation (GHI), c) Wind velocity.

Table 1
Physical and thermal properties of the pavement used in Eq. (1)[*] [2,20,21].

Independent Parameters			Dependent Parameters		
Parameter	Value	Unit	Parameter	Value	Unit
α	0.7	1	h	4.73	$BTU/(ft^2 \cdot hr \cdot °F)$
k	0.98	$BTU/(ft \cdot hr \cdot °F)$	D	0.031	ft^2/hr
Cp	0.21	$BTU/(lb \cdot °F)$	H	4.82	ft^{-1}
ρ	150	lb/ft^3	C	2.05	ft^{-1}
W	TMY3	mph	F	0.67	1

[*] Considering the constants presented in Eq. (1), these parameters are presented only in the US customary units.
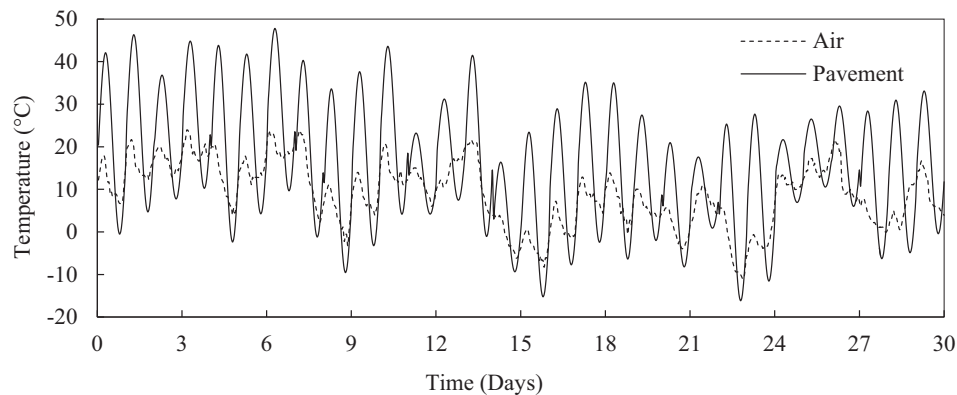

Fig. 2. Air temperature vs. pavement's surface temperature for the month of November in Lexington, KY.

PCM percentage. Details regarding the calculation of thermal properties of PCM impregnated concrete, as well as PCM's phase transition modeling is provided in another study [6].

The pavement cross-section was modeled as a multi-layer media, i.e. concrete slab, subbase, and subgrade soil. A schematic view of the pavement layers is shown in Fig. 3a. The pavement layer dimensions were selected to represent typical conditions, such those reported in the California Concrete Pavement Guide [25]. The thermal properties of the materials that were used in the model are presented in Table 2.

In order to have a point of reference, a concrete slab with no PCM was studied. Then, in order to obtain the most effective arrangement for PCM incorporation, two different scenarios were considered. As the first scenario, 20 vol% PCM was uniformly incorporated through the entire concrete slab's thickness (Fig. 3a). However, In the second scenario, PCM was incorporated only in the top part of the concrete slab (Fig. 3b). In order to make the results comparable, equal concentrations of PCM were used in both scenarios.

In each scenario, in order to calculate the temperature profile in the concrete slab, the pavement surface temperature, which was calculated in the previous section, was applied to the surface of the concrete slab, i.e. Point A in Fig. 3-a and -b.

The main parameter that causes curling stresses in a concrete slab is the temperature difference between the top and bottom surfaces of the slab. Therefore, this temperature difference was calculated in each scenario. The melting point of the PCM was selected to be equal to the average surface temperature, i.e. 15.8 °C. The specific heat and latent heat of fusion of the PCM were selected to be equal to 2.08 J/g·K and 200 J/g, respectively [26]. These parameters represent the thermal properties of a paraffin PCM with the number of carbon atoms between 14 and 18 [27].

2.3. Calculation of curling stresses in the concrete slab

In order to calculate the curling stresses that are induced in a concrete slab as a result of a temperature gradient, a 3-D finite ele-
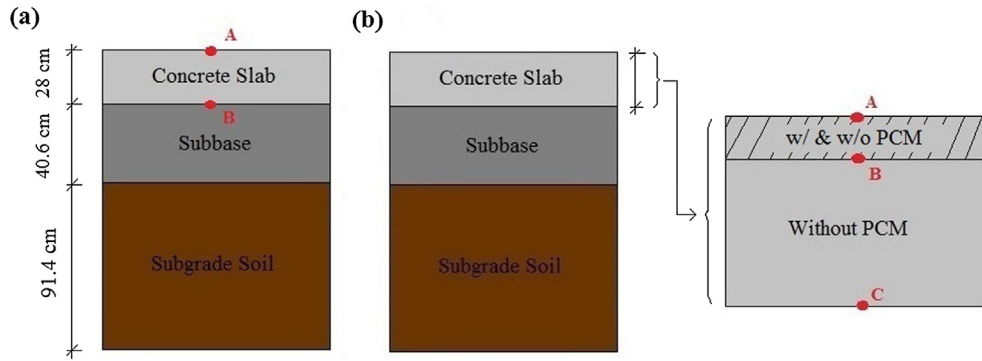
Fig. 3. Pavement's layers.

Table 2
Physical and thermal properties of the pavement's layers [2,21].

Material	ρ kg/m^3	Cp $J/g \cdot K$	k $W/m \cdot K$	Coefficient of thermal expansion $1/K$	Surface emissivity	E MPa	v
Concrete Slab	2400	0.88	1.20	13×10^{-6}	0.94	26,000	0.2
Subbase	2300	0.88	0.96	13×10^{-6}	0.92	8000	0.26
Subgrade Soil	1600	0.80	0.92	10×10^{-6}	0.92	80	0.28

ment stress analysis model using COMSOL software was employed. The model contained layers with different thermal and physical properties. Heat conduction in solids, and solid mechanics were the physics that were involved in the simulation. The schematic of the 3-D model of the pavement is shown in Fig. 4. It contains three layers: a 91.4 cm Subgrade Soil layer, a 40.6 cm Subbase layer, and a 28 cm Concrete Slab layer. In this model, the displacement in the three spatial directions of the lower level of the Subgrade Soil layer is fully restrained. However, the displacement of the upper level of this layer was not restrained. The displacements of the Subbase layer were not restrained, however, the displacement of the lower level of this layer was locked to the displacement of the upper level of the Subgrade Soil layer.

Temperature-induced curling in the concrete slab causes a discontinuity between the slab and the supporting subbase layer underneath [15]. Special consideration was given in the modeling of the slab to capture this phenomenon. Because of that, the displacement of the slab was not locked to the displacement of the Subbase layer. However, because of the symmetry, the displacements of the central point of the slab in the x- and y-directions were restrained.

In this research, the model was studied solely under thermal loads, and traffic loads were not applied. Temperatures with

Fig. 4. Three-D stresses analysis COMSOL model. Section A-A presents the location of Points U and L in the concrete slab.

different magnitudes were applied to different surface boundaries of the model, and the induced internal stresses at different points of the domain were calculated. In order to validate the accuracy of the model, the results of this study were compared with other studies that investigated the temperature induced stresses in concrete pavements. In one of the studies, finite element modeling was adopted [28], and in the other one a field study approach was used to measure concrete pavement responses to temperature-induced stresses [29].

2.3.1. Model validation 1

Faraggi et al. used finite element modeling to study the curling stresses in concrete pavements [28]. Their model consisted the following layers:

- Concrete slab: 4.57 m × 3.66 m × 25 cm, with E = 33 GPa
- Cement treated base: 30 cm thick, with E = 20 GPa
- Soil sub-base: 1 m thick, with E = 80 MPa.

They studied the model under two temperature gradients that were applied to the concrete slab: ΔT = −0.4 °C/cm, and ΔT = +0.6 °C/cm. A positive temperature gradient means that the top face of the slab is warmer than the bottom face. To validate the accuracy of the COMSOL model which was used in this study, two 3-D stress analysis models of pavements with similar layers were created, and similar temperature gradients. i.e. −0.4 °C/cm and +0.6 °C/cm, were applied to the concrete slabs. Since the boundary conditions were not completely explained in Faraggi's study, the modeling of the base and sub-base layers were conducted in such a manner that the supporting pavement layers were one meter wider than the slab above. This was done in order to minimize the potential for development of any complex boundary conditions along the edges of the slab. The results of this validation analysis are provided later in this paper.

2.3.2. Model validation 2

In another study, Yu et al. analyzed concrete pavement responses to temperature induced stresses which were measured via instrumented slabs [29]. In their study, the deformation responses of a concrete pavement with the following layers
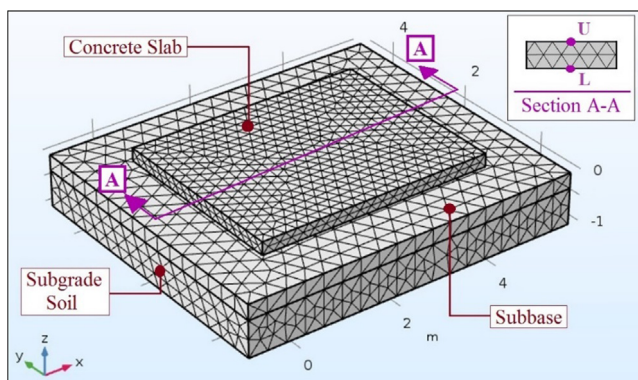
were measured when it was subjected to $\Delta T = -6.7\,°C$ and $\Delta T = +12.8\,°C$:

- Concrete slab: 4.7 m × 3.7 m × 29.2 cm, with E = 20.7 GPa and $\upsilon = 0.15$
- Cement treated base: 7.8 cm thick, with E = 4.8 GPa and $\upsilon = 0.35$
- Soil sub-base: 1 m thick, with E = 48.9 MPa.

To validate the accuracy of the COMSOL model, two 3-D models of pavements with similar layers and similar temperature gradients, i.e. $-6.7\,°C$ and $+12.8\,°C$, and boundary conditions were created. The results of this validation analysis are provided later in this paper.

2.4. Fatigue models

The primary goal of this research was to demonstrate how the addition of PCMs to concrete overlays can mitigate thermal induced curling stresses in concrete pavements. Obviously, since the source of these stresses is weather related, these stresses have a cyclic nature. This means that the pavement goes under cyclic changes in temperature, and thus multiple cycles of curling stresses on a daily basis. This cyclic changes in stresses causes fatigue damage in concrete slabs. Similar to other fatigue sensitive materials, concrete will fail under cyclic tensile loads. The number of cycles that a concrete specimen can tolerate before it fails is a function of the stress level. Therefore, various correlations between the stress level and maximum tolerable cycles are suggested by various researchers. The most common version of such a correlation is known as S-N relationship (Stress-Number of Cycles).

In this study, three different S-N relationships were adopted to calculate the fatigue damage in concrete pavements. These relationships yield different number of cycles to failure for a given stress level. The first employed S-N relationship was suggested by Titus-Glover for the survival level of 80% [30]:

$$\log N_f = \left[\frac{\left(\frac{\sigma}{MOR} \right)^{-10.24}}{0.1156} \right]^{0.217} \tag{4-a}$$

where N_f is number of cycles to failure, σ is the amplitude of applied flexural stress in fatigue loading, and MOR is modulus of rupture of concrete.

Portland Cement Association (PCA) is also one of the sources that has recommended an S-N relationship [31]:

$$For \frac{\sigma}{MOR} \geqslant 0.55 : \log N_f = 11.737 - 12.077\left(\frac{\sigma}{MOR} \right)$$

$$For\, 0.45 < \frac{\sigma}{MOR} < 0.55 : N_f = \left(\frac{4.2577}{\sigma/MOR - 0.4325} \right)^{3.268} \tag{4-b}$$

$$For \frac{\sigma}{MOR} \leqslant 0.45 : N_f = Unlimited$$

The third employed S-N relationship was suggested by Oh [32]:

$$\log N_f = \frac{0.956 - \sigma/MOR}{0.0536} \tag{4-c}$$

For comparison purposes, these three S-N relationships are shown in Fig. 5.

Because a concrete pavement undergoes cyclic loads with different intensities, a model such as the Miner's rule should be used to superimpose the effect of these cyclic loads. Based on the Miner's rule, a material will fail if the Damage Index (DI) of that under cyclic loads reaches unity [33]:

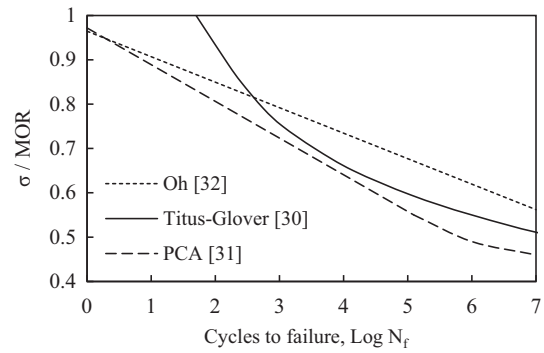$$DI = \sum_{i=1}^{N} \frac{n_i}{N_i} \tag{5}$$

Fig. 5. Comparison between three fatigue criteria for concrete.

where n_i is the number of cycles under a specific stress level that the specimen experiences, and N_i is the maximum number of cycles at that stress level that the specimen can tolerate before it fails. Eqs. 4(a)–4(c), and (5) were used to calculate the cumulative damage in concrete pavements under repetitive temperature gradient.

In order to calculate fatigue damage in concrete pavements due to thermal induced cyclic changes in curling stresses, and to evaluate the efficiency of PCMs to mitigate this deterioration mechanism, three models were generated. In the first model, a 28 cm concrete slab was considered (Fig. 3a). In the second model, a 7.6 cm thick concrete overlay was added on the top of the main slab without any PCM (Fig. 3b). Finally, the third model was identical to the second model, except 25 vol% PCM was added to the overlay (Fig. 3b). It should be mentioned that in the previous studies, the volume percentage of the incorporated PCM in concrete was suggested to be equal to 15% [34], 30% [24], 45% [2], and 57% [35]. The properties of pavement layers and the PCM are provided in Table 2.

Concrete overlays are considered as important preservation and rehabilitation methods for concrete and asphalt pavements [36]. They are categorized under resurfacing treatments, and can have the thickness of 5.1 cm to 25.4 cm [36]. Concrete overlays are divided in two categories: bonded and un-bonded overlay systems. In general, these systems are meant to add structural capacity and eliminate surface distresses on existing pavements, and to restore structural capacity to an existing pavement, respectively [36,37]. Other application of concrete overlays are designed for improving friction, noise, ride-ability, and eliminating rutting and shoving problems [36].

Various materials and additives such as steel and polypropylene fibers [38], and latex-modified concrete [39] are proposed to improve mechanical and chemical properties of concrete overlays. However, not enough attention has been devoted to the application of overlays to modify thermally induced distresses in pavements. Also, no additives have proposed to improve the thermal properties of the concrete overlays. In this study, PCMs are proposed as additives to improve the thermal properties of concrete overlays. The proposed PCM-rich concrete overlay should be constructed as a bonded overlay system, because if it is not bonded, the overlay and the main slab would curl independently. Thus, there would be times that gaps would form between the two layers, and the heat transfer between the layers would be interrupted. The application of an un-bonded PCM-rich concrete overlay in modifying thermally induced stresses in concrete slabs will be evaluated in future studies.

It should be mentioned that the design and construction considerations of the overlay are outside of the scope of this study. Detailed discussions regarding various carrier agents such as lightweight aggregate [26,40], rice husk ash [5], and high density

polyethylene balls [41], describing the incorporation methods of PCM in concrete have been provided in other studies. This research was aimed solely to study the effect of incorporating PCMs in a concrete overlay in order to reduce curling stresses.

For each of the aforementioned S-N models, the surface temperature of three cities in the US, with different climate parameters, were calculated by Eq. (1), and were applied to the top face of the concrete slab, and the following steps were taken to calculate the fatigue damage:

1- The heat transfer COMSOL model was used to calculate the hourly temperature profile of Point B, as shown in Fig. 3a, and Point B and Point C, as shown in Fig. 3b, for the entire year. Then, the temperature difference between Point A and Point B in Fig. 3a, and Point B and Point C in Fig. 3b, were calculated.
2- A MATLAB code was used to organized the temperature differences in eight categories, and to count the number of times that the temperatures difference falls in each of categories. These temperature categories cover a temperature range of −32 °C to +32 °C with temperature intervals of 8 °C. The average temperature of each category was considered as the representative-temperature of that category.
3- The 3-D stress analysis COMSOL model was used to calculate the induced curling stresses in the concrete slab for the representative-temperature of each category.
4- Finally, Eqs. (4) and (5) were used to calculate the damage indices in each case for one year.

To evaluate the efficiency of the proposed PCM-rich concrete overlay in different climates, three cities with different weather conditions were studied. These cities included Lexington, KY; Austin, TX; and Hancock, MI; which represent moderate, warm, and cold climates, respectively. The air temperature in these cities over the course of one full year is presented in Fig. 6. In order to better visualize the data, the polynomial (Poly) functions that were used to fit the average daily temperature of each city are presented. It should be mentioned that for each city, the performance of the proposed PCM-rich overlay would be different in different seasons of a year. Studying each case for one full year takes the effect of these seasonal variations into account, and yields a realistic evaluation of the performance of the proposed PCM-rich overlay.

3. Results and discussion

3.1. Concrete slab temperature gradient

To obtain the optimum placement for PCM in the slab cross-section, the temperature differences between the upper and lower
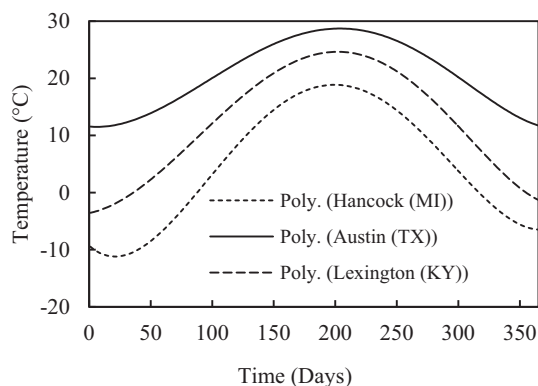
Fig. 6. Polynomial (Poly) function fitted to the average daily temperature profile of three different cities in the US.

levels of the concrete slab in two scenarios (addition of the PCM to the entire slab versus only to the top layer) were calculated.

3.1.1. Scenario 1: incorporating PCM in the entire concrete slab

The temperature differences for this scenario for the cases that 0 vol% PCM and 20 vol% PCM were incorporated in the concrete slab are shown in Fig. 7. Intuitively, one would expect that the PCM would ameliorate the temperature gradient which would in turn reduce the curling stresses in the slab. However, as it can be seen, the graph for the case of 20 vol% PCM does not exhibit a meaningful difference with the case of 0 vol% PCM.

In some rare combinations of time and temperature, the incorporation of PCM has even led to an increase in the temperature gradient in the concrete slab. For example, in day six, the absolute value of temperature difference increased by 3.2 °C. This is attributed to the increase in the thermal inertia of concrete slab when the PCM was incorporated in its entire mass.

In general, incorporating PCM in the entire slab was found not to be an effective strategy to decrease temperature gradient in concrete pavements. Curling stresses in a concrete slab are the result of temperature difference between upper and lower levels of the slab. Increasing slab's thermal inertia by incorporating PCMs does not effectively decrease the induced curling stresses.

3.1.2. Scenario 2: incorporating PCM in the top layer of the concrete slab

In the previous scenario, it was shown that the latent heat of fusion of a PCM does not work in the favor of modifying temperature gradient in a concrete slab when it is incorporated in the entire slab. However, the PCM could be effective when it is used in the top part of the slab. This leads to the idea of limiting the PCM to an overlay layer on the top of the concrete slab. In fact, in this scenario, the concrete slab is made of two layers, the main layer (the larger slab), which does not consist PCM, and an overlay that contains all of the PCM (Fig. 3b). By using an overlay arrangement, the use of PCM is isolated to the top portion of the slab, where the temperature changes on the upper level of the main slab (Point B in Fig. 3b) will be effectively moderated, while the thermal inertia of the main slab is not negatively altered. Both of these factors help to reduce the temperature gradient in the main slab.

To implement this idea, an overlay with the thickness of 7.6 cm was considered to include all the incorporated PCM. To make the analysis comparable with the case where the incorporated PCM was uniformly distributed in the entire thickness of the larger slab, the same concentration of PCM was used in the overlay. Surface temperature profile was applied to the pavement, i.e. Point A in Fig. 3b, and the temperature difference between the top and lower layers of the main slab, i.e. Point B and Point C in Fig. 3b, respectively, were calculated (Fig. 8). The findings show that the scenario 2, where all the PCM was incorporated in the overlay, was much more effective in modifying the temperature gradient in the main slab, and as a result, it was more effective in reducing curling stresses. On average, the positive temperature differences and the negative temperature differences were decreased by 5 °C and 6 °C, respectively. In some specific days, the temperature difference between Point B and Point C was almost negligible. This shows that the PCM-rich overlay can effectively control the temperature difference in the main slab. Additionally, as it is shown in the following sections, the concrete overlay without the PCM showed a limited capability to modify temperature gradient in the slab underneath, and the overlay with PCM played the key role in modifying temperature gradient in the slab. Therefore, enhancing the thermal inertia of a concrete overlay by incorporating PCMs in that layer seems to be an effective strategy to control temperature induced curling stresses in concrete pavements.
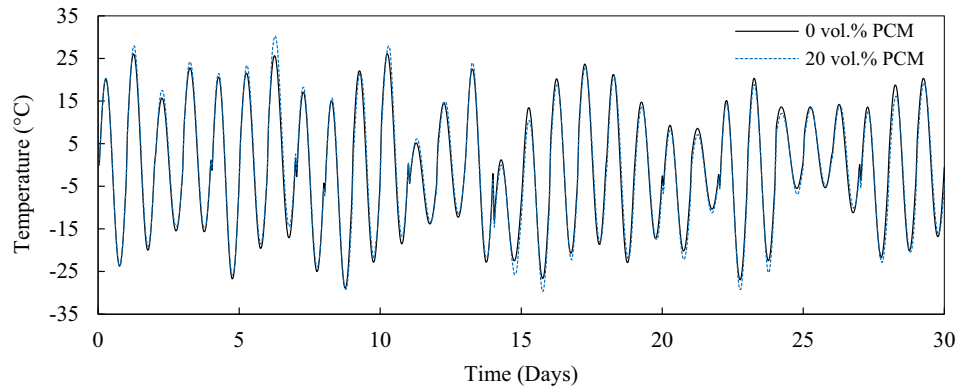
Fig. 7. Temperature difference between upper and lower level in the concrete slab for Scenario 1, month of November in Lexington, KY.
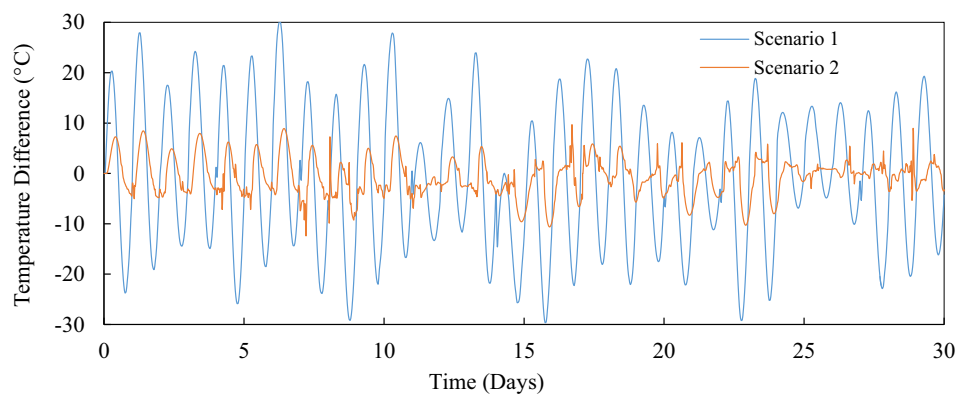

Fig. 8. Comparing efficiency of the two scenarios in modifying temperature difference in the main concrete layer. Equal amount of PCM was incorporated in each case.

3.2. Validation of the COMSOL stress analysis model

To validate the 3-D stress analysis model, the results were compared with two previous studies. In the first study, a pavement with three layers was modeled and two different temperature gradients. The deformed shape of the modeled pavement when negative temperature gradient was applied is shown in Fig. 9. As expected, a negative temperature gradient causes upward curling, and a positive temperature gradient causes downward curling [15]. As it has been discussed in the literature, when curling takes place in concrete pavements, the edges and the central point of the slab will be lifted during curling up and down, respectively. Hence there will be a discontinuity b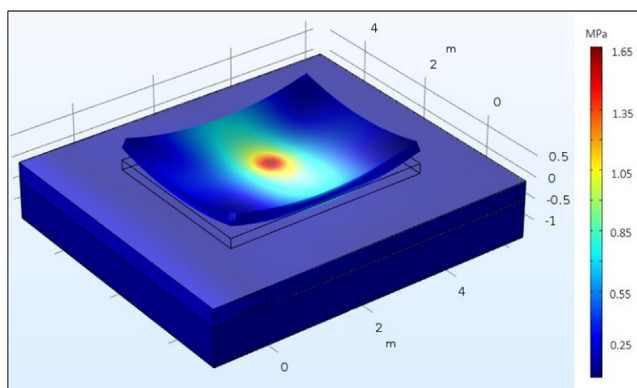etween the slab and the supporting sub-base layer underneath [15]. Special consideration was given in the modeling to capture this phenomenon in order to produce a realistic model that complies with what actually happens to a concrete slab in real conditions.

The comparison between the results obtained from the model and the results presented in the Faraggi *et al.*'s work [28] is presented in Table 3. These results present the stress condition at two different points on the top face of the slab. When the temperature gradient is negative, the top face of the slab contract, and the bottom face expands. This causes tensile (positive) stresses in the top face. However, when the temperature gradient is positive, the top face expands, and the bottom face contracts, which cases compressive (negative) stresses in the top face. Both of these stress conditions are caused by the force of gravity acting on the curled slab. As an example, tensile stresses in x- and y-directions of Points I, as defined in Table 3, under the temperature gradient of -0.4 °C/cm were reported to be equal to 1.72 MPa and 1.37 MPa, respectively [28]. The calculated stresses for these points using the COMSOL model were equal to 1.66 MPa and 1.45 MPa, which have an error of 3.5% and 5.8%, respectively. For Point I under the temperature gradient of $+0.6$ °C/cm, the error was about 5%. Some of the boundary conditions of the model were not explained in the reference [28], and reasonable assumptions were made to replicate their conditions in this study. The error that exists between the results are attributed to the differences in the boundary conditions.

The second study which was used for validation purposes was a field study [29]. In that study, the deformation of the slab was measured under positive and negative temperature gradients. The difference between maximum and minimum corner displacement was reported to be 1.07 mm [29]. Based on the results of the COMSOL modeling in this study, the upward displacement at the corner

Fig. 9. Deformed shape under negative temperature load of $\Delta T = -0.4$ (°C/cm).

Table 3
Comparison between the results presented by Faraggi et al. [28] and the COMSOL model.

Source	ΔT (°C/cm)							
	−0.4				+0.6			
	Point I[1]		Point II[2]		Point I[1]		Point II[2]	
	$\sigma_{x\ (MPa)}$	$\sigma_{y\ (MPa)}$	$\sigma_{x\ (MPa)}$	$\sigma_{y\ (MPa)}$	$\sigma_{x\ (MPa)}$	$\sigma_{y\ (MPa)}$	$\sigma_{x\ (MPa)}$	$\sigma_{y\ (MPa)}$
Faraggi et al.	1.72	1.37	0.75	0.00	−1.38	−0.76	−1.70	−0.06
This Study	1.66	1.45	0.71	0.00	−1.32	−0.81	−1.61	−0.06
Error%	3.5	5.8	5.3	0.0	4.3	6.6	5.3	0.0

[1] Center point of the slab's top face.
[2] Middle point of the longer edge of the slab's top face.

of slab under negative temperature gradient was 0.59 mm, and the downward displacement under positive gradient was 0.53 mm. The difference between these two displacements is 1.12 mm, which reflects 4% error when compared to the Yu et al. study [29]. These comparisons demonstrated that the model developed in this study was able to accurately calculate the induced curling stresses in a concrete pavement.

3.3. Fatigue analysis

A parametric study was performed in order to determine the relationship between the magnitude of applied temperature gradient and the resulting stresses in the concrete slab. The study was designed to apply the environmentally induced temperature gradients to the concrete slab in order to determine the resultant maximum bending tensile and compressive stresses on top and bottom faces of the slab. The maximum curling stresses occur at the center of the top and bottom surfaces of the slab (Points U and L in Fig. 4). These results are summarized in Fig. 10, which shows how the applied temperature gradient correlates with the induced stresses. Positive temperature difference means that the upper side of the slab is warmer than the lower side, and vice versa.

As one would expect, an increase in the temperature difference would cause an increase in the corresponding bending stresses; however, there is not a linear relationship between these two parameters. Since concrete is much weaker under tensile stress as compared to compressive stress, the upper part of the graph is the critical zone. Additionally, since Point U experiences higher tensile stresses as compared to Point L, it is the critical point with respect to the accumulation of fatigue damage.

A comprehensive fatigue study was carried out to evaluate the effectiveness of the PCM-rich concrete overlay in controlling the thermal induced curling stresses in concrete pavements. Three different fatigue models were adopted. For each model, the fatigue

Fig. 10. Induced tensile and compressive stresses in the slab for different temperature differences.

analysis was carried out for three cities, and for each city, three slab cases were studied. In the first slab case, no concrete overlay was used. In the second and third slab cases, a 7.6 cm concrete slab with 0 vol% PCM and 25 vol% PCM were considered on the top of concrete slab, respectively.

Since the magnitude of induced curling stress is a function of the magnitude of temperature difference between top and bottom faces of the concrete slab, the range of temperature difference for each slab case was divided in eight categories. For each category, the induced tensile stress at Points U and L for the corresponding temperature difference representative was calculated. Also, the occurrence frequency of that temperature category during one full year was calculated (Table 4). The Modulus of Rupture (MOR) of the concrete was considered to be 4.5 MPa (AASHTO T 97), and the fatigue stress ratio, which is the tensile stress divided by MOR, for each category was calculated.

3.3.1. Fatigue analysis based on equation suggested by Titus-Glover [30]

The temperature data for the first geographic location, the city of Lexington, KY, was studied for one full year. Table 4 presents the occurrence frequency for each temperature category for this city and for one full year. It also presents the fatigue damage index of the slab for each year. For the slab case without overlay (Fig. 3a), the DI was calculated to be equal to 0.00455 per year. This means that if the service life of a pavement is considered to be equal to 35 years, the cumulative DI of the pavement is 0.16. It should be mentioned that this is the damage that is solely produced because of thermally-induced curling stresses. Other sources of damage in concrete pavements, such as traffic load and freeze/thaw induced deterioration, should be added up to this damage index. Damage factors due to factors other than curling are outside of the scope of this study. The focus of this research was to study the effectiveness of a PCM-rich overlay in ameliorating the curling stresses.

For the slab case with a 7.6 cm concrete overlay and without PCM curling stresses were calculated (Table 5). As expected, the temperature difference was moderated, and it never reached to −28 °C category. However, it frequently reached to −20 °C category. The overlay was able to bring the DI down to 0.00229 per year. Considering the same 35-year service life for the concrete slab, the cumulative DI would be equal to 0.08. This shows that a concrete overlay without PCM can reduce the curling-induced fatigue damage; however, a conventional bonded overlay without PCM is not as effective as a PCM-rich overlay, as it is described in the following section.

The third slab case involved a PCM-rich concrete overlay (25 vol% PCM), and curling stress data are reported in Table 6. As the results in Table 6 show, the temperature difference never reached to the −28 °C category, and it rarely reached to the −20 °C category. In this slab case, the DI was as low as 0.00009 per year, which leads to the cumulative DI equal to 0.0031 after 35 years. This is a very low DI, and it suggests that the PCM-rich overlay was able to
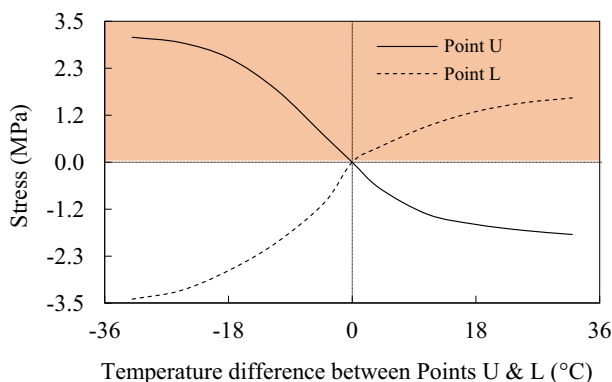
Table 4
Fatigue deterioration in the slab that does not have an overlay, Lexington, KY, Titus-Glover fatigue equation.

Range of temp. difference between points U & L (°C)	Temp. difference representative (°C)	Equivalent tensile stress (MPa)	Point under tensile stress	Occurrence Frequency in one year	Normalized to flexural strength	Fatigue Damage	
						N_f	DI per year
−32 to −24	−28	2.98	U	109	0.63	24896	0.00438
−24 to −16	−20	2.60	U	151	0.55	896779	0.00017
−16 to −8	−12	2.03	U	88	0.39	N/A	–
−8 to 0	−4	0.48	U	17	0.10	N/A	–
0 to 8	4	0.38	L	38	0.08	Sum:	0.00455
8 to 16	12	0.91	L	85	0.19		
16 to 24	20	1.26	L	124	0.27		
24 to 32	28	1.48	L	118	0.31		

Table 5
Fatigue deterioration in the slab that has an overlay with 0 vol% PCM, Lexington, KY, Titus-Glover fatigue equation.

Range of temp. difference between points U & L (°C)	Temp. difference representative (°C)	Equivalent tensile stress (MPa)	Point under tensile stress	Occurrence Frequency in one year	Normalized to flexural strength	Fatigue Damage	
						N_f	DI per year
−32 to −24	−28	N/A	U	0	N/A	N/A	–
−24 to −16	−20	2.84	U	178	0.60	78025	0.00228
−16 to −8	−12	2.35	U	149	0.50	3.E + 07	0.00001
−8 to 0	−4	0.86	U	38	0.18	N/A	–
						Sum:	0.00229

Table 6
Fatigue deterioration in the slab that has an overlay with 25 vol% PCM, Lexington, KY, Titus-Glover fatigue equation.

Range of temp. difference between points U & L (°C)	Temp. difference representative (°C)	Equivalent tensile stress (MPa)	Point under tensile stress	Occurrence Frequency in one year	Normalized to flexural strength	Fatigue Damage	
						N_f	DI per year
−32 to −24	−28	N/A	U	0	N/A	N/A	–
−24 to −16	−20	2.80	U	10	0.60	111916	0.00009
−16 to −8	−12	2.28	U	252	0.49	9.E + 07	0.00000
−8 to 0	−4	0.81	U	103	0.17	N/A	–
						Sum:	0.00009

effectively minimize the fatigue damage due to thermally-induced curling stresses.

The reduction in DI when PCM was incorporated in the overlay was about three times higher than the case without PCM. The results of other simulations show that in order to achieve the same level of fatigue damage reduction without PCM in the overlay, the thickness of the overlay should be raised to 12.7 cm, which is 5.1 cm thicker than the overlay that contained PCM.

Similar calculations were carried out for the city of Austin, TX, which represents a relatively warmer climate compared to the other two geographical locations in this study. For this city and for the case of no overlay, the DI for one year was 0.00641 which leads to a cumulative DI of 0.22 during the service life pavement (Table 7). When the concrete overlay with 0 vol% PCM was applied,

the DI was reduced to 0.00303 per year, which leads to 0.11 cumulative DI for the service life of the pavement. This shows a 51% reduction in the DI when overlay with no PCM was used. However, when 25 vol% PCM was incorporated in the overlay, the DI was reduced to 0.00012 per year, which leads to cumulative DI of 0.0042. This means a 98% reduction in the DI resulted from temperature-induced curling stresses. The results also suggest that by incorporating 25 vol% PCM in the overlay, the effectiveness of the overlay for reducing curling-induced fatigue damage was doubled when compared to the overlay without the PCM (Table 8).

Finally, the city of Hancock, MI, was studied. For this city, DI per year was equal to 0.00557 for the case of a slab with no overlay, and thus cumulative DI was equal to 0.19. When 0 vol% PCM overlay was applied, the cumulative DI year was reduced to 0.07, which

Table 7
Fatigue deterioration in the slab for different overlay condition, Austin, TX, Titus-Glover fatigue equation.

Range of temp. difference between points U & L (°C)	With no overlay		With 0 vol% PCM overlay		With 25 vol% PCM overlay	
	Occurrence Frequency in one year	DI per year	Occurrence Frequency in one year	DI per year	Occurrence Frequency in one year	DI per year
−32 to −24	156	0.00627	0	–	0	–
−24 to −16	131	0.00015	188	0.00303	15	0.00012
−16 to −8	58	–	135	0.00000	244	0.00000
−8 to 0	20	–	42	–	106	–
	Sum:	0.00641	Sum:	0.00303	Sum:	0.00012

means a 62% reduction. However, when the PCM-rich overlay was applied, the cumulative DI was reduced to 0.0024, which means a 99% reduction. Subtracting 62% from 99% suggests that the net contribution of the PCM for reducing the deterioration resulted from repetitive curling stresses was up to 36%. These findings are in agreement with the results presented in another study regarding the fatigue life of concrete pavements under flexural loadings [42].

3.3.2. Fatigue analysis based on equations suggested by PCA [31] and Oh [32]

The results for the fatigue analysis based on the S-N relationship suggested by PCA are shown in Table 9. Similar evaluations were carried out to further verify the performance of the proposed PCM-rich concrete overlay. To avoid the repetition of detailed discussions, only the final results for each city are presented here. For the city of Lexington, the results show that the net contribution of the PCM in reducing the DI was 74%. Additionally, for the city of Austin and the city of Hancock, this contribution was 43% and 53%, respectively. These results suggest that based on the PCA fatigue model, the PCM in the concrete overlay was able to effectively moderate temperature gradients in the main concrete slab and thereby enhance the fatigue life of the concrete slab as related to curling stresses. Furthermore, comparing the Titus-Glover model with the PCA criteria suggest that the PCA fatigue model is very conservative. This in agreement with the results of other studies

where it was reported that the fatigue curve of PCA lies below most of other fatigue curves [43].

The results for the fatigue analysis based on the S-N relationship suggested by Oh are shown in Table 10.

As it can be seen in Fig. 5, the fatigue curve related to Oh's relationship is located above the other two curves, which means that for any given stress level, Oh's relationship predicts a much longer fatigue life (N_f). The data presented in Table 10 suggest that for all the three cities, even for the case without an overlay, the DI is a very small number based on the Oh's model (the cumulative damage in the service life of pavement would be less than 0.5%). This suggests that based on the Oh's fatigue criterion, which is not very conservative, curling stresses may not be a major factor for fatigue damage. However, using a concrete overlay with 25 vol% PCM would reduce the curling stresses to virtually a negligible level.

The fatigue analysis results suggest that regardless of the climate condition (warm, moderate, cold), the PCM-rich concrete overlay would be a reliable strategy to control curling stresses in concrete pavements and reduce curling-induced fatigue damage. It should also be added that the fluctuation of temperature gradients not only causes curling stresses in concrete pavements, but also causes loss of support at the slab edges and corners [15]. Therefore, using a PCM-rich overlay may have beneficial outcomes beyond the reduction of curling-induced fatigue.

Table 8
Fatigue deterioration in the slab for different overlay condition, Hancock, MI, Titus-Glover fatigue equation.

Range of temp. difference between points U & L (°C)	With no overlay		With 0 vol% PCM overlay		With 25 vol% PCM overlay	
	Occurrence Frequency in one year	DI per year	Occurrence Frequency in one year	DI per year	Occurrence Frequency in one year	DI per year
−32 to −24	135	0.00542	0	–	0	–
−24 to −16	128	0.00014	155	0.00207	7	0.00007
−16 to −8	69	–	157	0.00001	238	0.00000
−8 to 0	33	–	53	–	120	–
	Sum:	0.00557	Sum:	0.00208	Sum:	0.00007

Table 9
Fatigue deterioration in the slab based on PCA fatigue equation.

Range of temp. difference between points U & L (°C)	DI per year								
	Lexington (KY)			Austin (TX)			Hancock (MI)		
	No overlay	Overlay with 0 vol% PCM	Overlay with 20 vol% PCM	No overlay	Overlay with 0 vol% PCM	Overlay with 20 vol% PCM	No overlay	Overlay with 0 vol% PCM	Overlay with 20 vol% PCM
−32 to −24	0.00811	–	–	0.01160	–	–	0.01004	–	–
−24 to −16	0.00121	0.00709	0.00028	0.00105	0.00702	0.00040	0.00103	0.00601	0.00019
−16 to −8	–	0.00020	0.00015	–	0.00018	0.00016	–	0.00021	0.00014
−8 to 0	–	–	–	–	–	–	–	–	–
Sum:	0.00932	0.00729	0.00043	0.01266	0.00720	0.00056	0.01107	0.00622	0.00034

Table 10
Fatigue deterioration in the slab based on Oh fatigue equation.

Range of temp. difference between points U & L (°C)	DI per year								
	Lexington (KY)			Austin (TX)			Hancock (MI)		
	No overlay	Overlay with 0 vol% PCM	Overlay with 20 vol% PCM	No overlay	Overlay with 0 vol% PCM	Overlay with 20 vol% PCM	No overlay	Overlay with 0 vol% PCM	Overlay with 20 vol% PCM
−32 to −24	0.00009	–	–	0.00013	–	–	0.00011	–	–
−24 to −16	0.00000	0.00005	0.00000	0.00000	0.00006	0.00000	0.00000	0.00004	0.00000
−16 to −8	–	0.00000	0.00000	–	0.00000	0.00000	–	0.00000	0.00000
−8 to 0	–	–	–	–	–	–	–	–	–
Sum:	0.00009	0.00005	0.00000	0.00013	0.00006	0.00000	0.00012	0.00004	0.00000

4. Conclusion and future work

In this study, the ability of a PCM-rich concrete overlay in reducing curling stresses in concrete pavements was studied. In concrete pavements, temperature gradient through the slab causes curling stresses, which are comparable to the stresses that are induced by traffic loads. The results of this study show that by increasing the temperature gradient, the induced stresses increase; however, there is not a linear relationship between these two parameters. The thermally-induced curling stresses have a cyclic nature, and thus causes fatigue damage in concrete pavements. It was shown that the cumulative fatigue damage index resulted from curling stresses in a concrete pavement without a PCM-rich overlay could reach to up to 22% over the course of the service life. However, using a 7.6 cm bonded concrete overlay with 25 vol% PCM on the top of a concrete slab can effectively reduce this damage, and thus increase the service life of the pavement. This idea can be considered as a pavement preservation strategy for concrete pavements that are slated for an overlay treatment. Alternatively, the PCM-rich concrete overlay can be applied as a protective layer to a newly constructed concrete pavement in order to extend the service life of the pavement.

Conflict of interest

The authors declare no conflict of interest.

References

[1] D. Zhou, C.-Y. Zhao, Y. Tian, Review on thermal energy storage with phase change materials (PCMs) in building applications, Appl. energy 92 (2012) 593–605.
[2] D.P. Bentz, R. Turpin, Potential applications of phase change materials in concrete technology, Cem. Concr. Compos. 29 (7) (2007) 527–532.
[3] S. Raoux, Phase change materials, Annu. Rev. Mater. Res. 39 (2009) 25–48.
[4] B. Zalba et al., Review on thermal energy storage with phase change: materials, heat transfer analysis and applications, Appl. Therm. Eng. 23 (3) (2003) 251–283.
[5] N.P. Sharifi et al., Application of lightweight aggregate and rice husk ash to incorporate phase change materials into cementitious materials, J. Sustainable Cem.-Based Mater. 5 (6) (2016) 349–369.
[6] N.P. Sharifi, A.A.N. Shaikh, A.R. Sakulich, Application of phase change materials in gypsum boards to meet building energy conservation goals, Energy Build. 138 (2017) 455–467.
[7] N. Soares et al., Review of passive PCM latent heat thermal energy storage systems towards buildings' energy efficiency, Energy Build. 59 (2013) 82–103.
[8] J. Kosny et al., Theoretical and Experimental Thermal Performance Analysis of Complex Thermal Storage Membrane Containing Bio-Based Phase Change Material (PCM), Oak Ridge National Laboratory (ORNL); Building Technologies Research and Integration Center, 2010.
[9] M. Chen, L. Wan, J. Lin, Effect of phase-change materials on thermal and mechanical properties of asphalt mixtures, J. Test. Eval. 40 (5) (2012) 746–753.
[10] Y. Farnam et al., Evaluating the use of phase change materials in concrete pavement to melt ice and snow, J. Mater. Civ. Eng. 28 (4) (2015) 04015161.
[11] M.Z. Chen et al., Optimization of phase change materials used in asphalt pavement to prevent rutting, Advanced Materials Research, Trans Tech Publ, 2011.
[12] B. Guan, B. Ma, F. Qin, Application of asphalt pavement with phase change materials to mitigate urban heat island effect, in: Water Resource and Environmental Protection (ISWREP), 2011 International Symposium on 2011. IEEE.
[13] T. Karlessi et al., Development and testing of PCM doped cool colored coatings to mitigate urban heat island and cool buildings, Build. Environ. 46 (3) (2011) 570–576.
[14] C. Channakeshava, F. Barzegar, G.Z. Voyiadjis, Nonlinear FE analysis of plain concrete pavements with doweled joints, J. Transp. Eng. 119 (5) (1993) 763–781.
[15] H.T. Yu, L. Khazanovich, M.I. Darter, Consideration of JPCP curling and warping in the 2002 design guide, in: 83rd Annual Meeting of the Transportation Research Board, Washington, DC, 2004.
[16] K.C. Mahboub, Y. Liu, D.L. Allen, Evaluation of temperature responses in concrete pavement, J. Transp. Eng. 130 (3) (2004) 395–401.
[17] K.C. Mahboub, D.L. Allen, Y. Liu, A 3-D Finite Element Structural Model of an Instrumental Rigid Pavement (I-265 Gene Snyder Freeway, Louisville, Kentucky), 2002.
[18] Typical Meteorological Year, Available from: <http://rredc.nrel.gov/solar/old_data/nsrdb/1991-2005/tmy3/>.
[19] D.P. Bentz, A computer model to predict the surface temperature and time-of-wetness of concrete pavements and bridge decks, 2000.
[20] Y. Qin, Pavement surface maximum temperature increases linearly with solar absorption and reciprocal thermal inertial, Int. J. Heat Mass Transf. 97 (2016) 391–399.
[21] E.S. Barber, Calculation of maximum pavement temperatures from weather reports, Highway Res. Board Bull. (1957). 168.
[22] H.S. Esmaeeli et al., Numerical analysis of the freeze-thaw performance of cementitious composites that contain phase change material (PCM), Mater. Des. 145 (2018) 74–87.
[23] A.P. Carman, R.A. Nelson, Thermal Conductivity and Diffusivity of Concrete, University of Illinois at Urbana Champaign, College of Engineering Engineering Experiment Station, 1921.
[24] N.P. Sharifi, G.E. Freeman, A.R. Sakulich, Using COMSOL modeling to investigate the efficiency of PCMs at modifying temperature changes in cementitious materials–case study, Constr. Build. Mater. 101 (2015) 965–974.
[25] State of California Department of Transportation, Concrete Pavement Guide, 2015.
[26] N.P. Sharifi, A. Sakulich, Application of phase change materials to improve the thermal performance of cementitious material, Energy Build. 103 (2015) 83–95.
[27] A. Sharma et al., Review on thermal energy storage with phase change materials and applications, Renewable Sustainable Energy Rev. 13 (2) (2009) 318–345.
[28] V. Faraggi, C. Jofré, C. Kraemer, Combined effect of traffic loads and thermal gradients on concrete pavement design, Transp. Res. Rec. 1136 (1987) 108–118.
[29] H. Yu et al., Analysis of concrete pavement responses to temperature and wheel loads measured from intrumented slabs, Transp. Res. Rec.: J. Transp. Res. Board 1639 (1998) 94–101.
[30] L. Titus-Glover et al., Enhanced portland cement concrete fatigue model for streetpave, Transp. Res. Rec.: J. Transp. Res. Board 1919 (2005) 29–37.
[31] R.G. Packard, S.D. Tayabji, New PCA thickness design procedure for concrete highway and street pavements, in: Third International Conference on Concrete Pavement Design and RehabilitationPurdue University; Federal Aviation Administration; and Indiana Department of Highways, 1985.
[32] B.H. Oh, Fatigue analysis of plain concrete in flexure, J. Struct. Eng. 112 (2) (1986) 273–288.
[33] R. Tepfers, C. Fridén, L. Georgsson, A study of the applicability to the fatigue of concrete of the Palmgren-Miner partial damage hypothesis, Mag. Concr. Res. 29 (100) (1977) 123–130.
[34] A.R. Sakulich, D.P. Bentz, Increasing the service life of bridge decks by incorporating phase-change materials to reduce freeze-thaw cycles, J. Mater. Civ. Eng. 24 (8) (2011) 1034–1042.
[35] R. Baetens, B.P. Jelle, A. Gustavsen, Phase change materials for building applications: a state-of-the-art review, Energy Build. 42 (9) (2010) 1361–1368.
[36] K. Smith, et al., Concrete Pavement Preservation Guide, 2014.
[37] L.B. Heckel, Performance of an unbonded concrete overlay on I-74, 2002.
[38] M.O. Kim, A.C. Bordelon, Age-dependent properties of fiber-reinforced concrete for thin concrete overlays, Constr. Build. Mater. 137 (2017) 288–299.
[39] M.M. Sprinkel, Twenty-year performance of latex-modified concrete overlays, Polymer-Modified Hydraulic-Cement Mixtures, ASTM International, 1993.
[40] A.R. Sakulich, D.P. Bentz, Incorporation of phase change materials in cementitious systems via fine lightweight aggregate, Constr. Build. Mater. 35 (2012) 483–490.
[41] V. Tyagi et al., Thermodynamics and performance evaluation of encapsulated PCM-based energy storage systems for heating application in building, J. Therm. Anal. Calorim. 115 (1) (2014) 915–924.
[42] M. Lee, B. Barr, An overview of the fatigue behaviour of plain and fibre reinforced concrete, Cem. Concr. Compos. 26 (4) (2004) 299–305.
[43] Y.H. Huang, Pavement analysis and design. 2004.